



Mesenchymal Stem-Like Cells Derived from the Ventricle More Effectively Enhance Invasiveness of Glioblastoma Than Those Derived from the Tumor

Junseong Park^{1,2*}, Dongkyu Lee^{1,3*}, Jin-Kyoung Shim^{1,3}, Seon-Jin Yoon^{1,4}, Ju Hyung Moon¹, Eui Hyun Kim^{1,3}, Jong Hee Chang¹, Su-Jae Lee⁵, and Seok-Gu Kang^{1,3,6}

¹Department of Neurosurgery, Brain Tumor Center, Severance Hospital, Yonsei University College of Medicine, Seoul;

²Precision Medicine Research Center, College of Medicine, The Catholic University of Korea, Seoul;

³Brain Tumor Translational Research Laboratory, Avison Biomedical Research Center, Yonsei University College of Medicine, Seoul;

⁴Department of Biochemistry and Molecular Biology, College of Medicine, Yonsei University, Seoul;

⁵Fibrosis and Cancer Targeting Biotechnology, FNCT Biotech, Seoul;

⁶Department of Medical Science, Yonsei University Graduate School, Seoul, Korea.

Purpose: Glioblastoma (GBM) is one of the most lethal human tumors with a highly infiltrative phenotype. Our previous studies showed that GBM originates in the subventricular zone, and that tumor-derived mesenchymal stem-like cells (tMSLCs) promote the invasiveness of GBM tumorspheres (TSs). Here, we extend these studies in terms of ventricles using several types of GBM patient-derived cells.

Materials and Methods: The invasiveness of GBM TSs and ventricle spheres (VSs) were quantified via collagen-based 3D invasion assays. Gene expression profiles were obtained from microarray data. A mouse orthotopic xenograft model was used for in vivo experiments.

Results: After molecular and functional characterization of ventricle-derived mesenchymal stem-like cells (vMSLCs), we investigated the effects of these cells on the invasiveness of GBM TSs. We found that vMSLC-conditioned media (CM) significantly accelerated the invasiveness of GBM TSs and VSs, compared to the control and even tMSLC-CM. Transcriptome analyses revealed that vMSLC secreted significantly higher levels of several invasiveness-associated cytokines. Moreover, differentially expressed genes between vMSLCs and tMSLCs were enriched for migration, adhesion, and chemotaxis-related gene sets, providing a mechanistic basis for vMSLC-induced invasion of GBM TSs. In vivo experiments using a mouse orthotopic xenograft model confirmed vMSLC-induced increases in the invasiveness of GBM TSs.

Conclusion: Although vMSLCs are non-tumorigenic, this study adds to our understanding of how GBM cells acquire infiltrative features by vMSLCs, which are present in the region where GBM genesis originates.

Key Words: Glioblastoma, tumor invasion, mesenchymal stem-like cell, subventricular zone, patient-derived tumorsphere, ventricle-derived mesenchymal stem-like cells

Received: September 27, 2022 **Revised:** January 2, 2023

Accepted: January 5, 2023 **Published online:** February 7, 2023

Corresponding author: Seok-Gu Kang, MD, PhD, Department of Neurosurgery, Brain Tumor Center, Severance Hospital, Yonsei University College of Medicine, 50-1 Yonsei-ro, Seodaemun-gu, Seoul 03722, Korea.

E-mail: seokgu9@gmail.com

*Junseong Park and Dongkyu Lee contributed equally to this work.

•The authors have no potential conflicts of interest to disclose.

© Copyright: Yonsei University College of Medicine 2023

This is an Open Access article distributed under the terms of the Creative Commons Attribution Non-Commercial License (<https://creativecommons.org/licenses/by-nc/4.0>) which permits unrestricted non-commercial use, distribution, and reproduction in any medium, provided the original work is properly cited.

INTRODUCTION

Glioblastoma (GBM), the most common primary brain tumor, is a highly aggressive malignancy with poor prognosis,¹ despite multimodal treatment with surgery, radiotherapy, and chemotherapy.²⁻⁴ High-grade GBM exhibits a devastating malignant progression, characterized by resistance to conventional therapies and an infiltrative, progressive nature.^{5,6} A major barrier to the effective treatment of GBM is invasion of tumor cells into normal brain area. It has been reported that these malignant characteristics of GBM are related to the presence of stem-like

cells at the invasive front,⁷ as represented in vitro by GBM tumorspheres (TSs).⁸ Accordingly, in this study, we utilized GBM patient-derived primary TSs and their mouse orthotopic xenograft models, which have been highlighted as good model platforms for testing drug effects and characterizing specific features of GBM, including stemness and invasiveness.⁹⁻¹²

Although there have been many attempts to develop novel therapeutic strategies, these efforts have failed to improve the overall survival of GBM patients,¹³ highlighting the urgent need for new conceptual approaches to overcome treatment failure. During the invasion process, GBM cells interact with a variety of extracellular matrix (ECM) molecules;^{14,15} thus, targeting ECM and stromal factors has recently emerged as a therapeutic strategy for circumventing the malignant behavior of GBM.¹⁶ Mesenchymal stem cells (MSCs), typically isolated from bone marrow and well-known as multipotent precursors, could be plausible target in this regard, since mesenchymal stem-like cells (MSLCs) have been detected in brain tumors and recognized to play important roles in the tumor microenvironment.¹⁷⁻¹⁹ We also reported that tumor-derived MSLCs (tMSLCs) promote the invasiveness of GBM through the C5a/p38 MAPK/ZEB1 axis,²⁰ establishing tMSLCs as prognostic indicators²¹ and potential novel therapeutic targets in the stroma.

Our previous studies suggested the subventricular zone (SVZ), which is distinct from the tumor region, as the origin of GBM.²²⁻²⁴ Notably, MSLCs have also been isolated from ventricles; however, participation of these ventricle-derived MSLCs (vMSLCs) in cancer progression remains largely unexplored. Similar to the case for tMSLCs, we hypothesized that vMSLC are capable of promoting the invasion of GBM and are associated with poor prognosis. Here, we evaluated the contribution of vMSLCs to the invasiveness of GBM TSs and ventricle spheres (VSs) and sought to elucidate the molecular mechanisms underlying their pathological roles.

MATERIALS AND METHODS

Patient information and MR images

A total of seven *IDH1* wild-type GBM patients, newly diagnosed without a prior history of treatment with surgery, chemotherapy, or radiotherapy, were included in this study (Table

1). MR images of patients were taken using Achieva 3.0T system (Philips Medical Systems, Best, The Netherlands) 7 days or less before removal of the respective brain tumor. Axial images were planned parallel to the anterior and posterior limb of the corpus callosum. This study was performed in line with the principles of the Declaration of Helsinki. Approval was granted by the Institutional Review Board of Severance Hospital, Yonsei University College of Medicine (4-2012-0212, 4-2014-0649).

Isolation of GBM TSs, VSs, tMSLCs, and vMSLCs

Patient-derived GBM cells were established from fresh tissue specimens, as previously described.¹⁰ For culture of GBM TS and VS,^{12,25,26} cells were cultured in TS complete medium, composed of DMEM/F-12 (Mediatech, Manassas, VA, USA), 1x B27 (Invitrogen, San Diego, CA, USA), 20 ng/mL bFGF, and 20 ng/mL EGF (Sigma-Aldrich, ST. Louis, MO, USA). For culture of tMSLC and vMSLC, cells were cultured in MSC complete medium consisting of MEM α , 10% FBS (Lonza, Basel, Switzerland), 2 mM L-glutamine (Mediatech), and 100x antibiotic-antimycotic solution (Gibco, Gaithersburg, MD, USA). For generation of MSLC-conditioned media (CM), medium was changed from MSC complete medium to TS complete medium when MSLCs had adhered to the dish and reached >70% confluence. MSLC-cultured TS complete medium was collected after 48 h, and centrifuged to exclude cell debris. Characterization of MSLCs with respect to morphology, marker expression, mesenchymal differentiation, and tumorigenesis were performed as previously described.¹⁷ The surface markers CD105, CD31, and CD90 (eBioscience, San Diego, CA, USA), and CD73, CD45, and NG2 (BD Pharmingen, San Jose, CA, USA) were detected using flow cytometry.

3D invasion assay

Each well of a 96-well plate was filled with matrix composed of Matrigel, collagen type I (Corning Incorporated, Tewksbury, MA, USA), and TS complete media. Single spheroids were seeded inside the matrix prior to gelation, after which TS complete media was applied over the gelled matrix to prevent drying. The invaded area was quantified as follows: occupied area at (72 h-0 h)/occupied area at 0 h.

Table 1. Clinical Characteristics of the Samples in This Study

Case	Used cell type	Sex	Age	<i>IDH1</i> mutation	<i>MGMT</i> promoter	1p/19q
09-03	tMSLC	M	39	Wild-type	Methylated	Intact
13-15	tMSLC, vMSLC	M	60	Wild-type	Unmethylated	Intact
14-15	TS	M	67	Wild-type	Methylated	Intact
14-46	tMSLC	M	61	Wild-type	Unmethylated	Intact
15-88	TS, VS	M	61	Wild-type	Unmethylated	Intact
16-27	vMSLC	M	50	Wild-type	Unmethylated	Intact
17-16	vMSLC	M	53	Wild-type	Methylated	Intact

tMSLC, tumor-derived mesenchymal stem-like cell; vMSLC, ventricle-derived mesenchymal stem-like cell; TS, tumorsphere; VS, ventricle sphere.

Gene expression microarray datasets and analysis

Total RNA was extracted from GBM TSs and their matched patient tissues using a Qiagen RNeasy Plus Mini kit according to the manufacturer’s protocol, and loaded onto an Illumina HumanHT-12 v4 Expression BeadChip (Illumina, San Diego, CA, USA). After applying a variance-stabilizing transformation, data were quantile-normalized using the R/Bioconductor lumi package.²⁷ Heat maps were generated using GENE-E software. Genes were functionally annotated by over-representation analysis using GO gene sets, and then visualized as an enrich-

ment map using Cytoscape with ClueGO²⁸ plug-in. Enriched GO terms were categorized according to their kappa scores (>0.4). Statistical significance was determined using a two-sided hypergeometric test, and only nodes with a Bonferroni-adjusted *p*-value<0.01 were displayed. The datasets generated during and/or analyzed during the current study are available from the corresponding author upon reasonable request.

Western blotting

Cell lysates were separated by SDS-PAGE on 10% Tris-Glycine

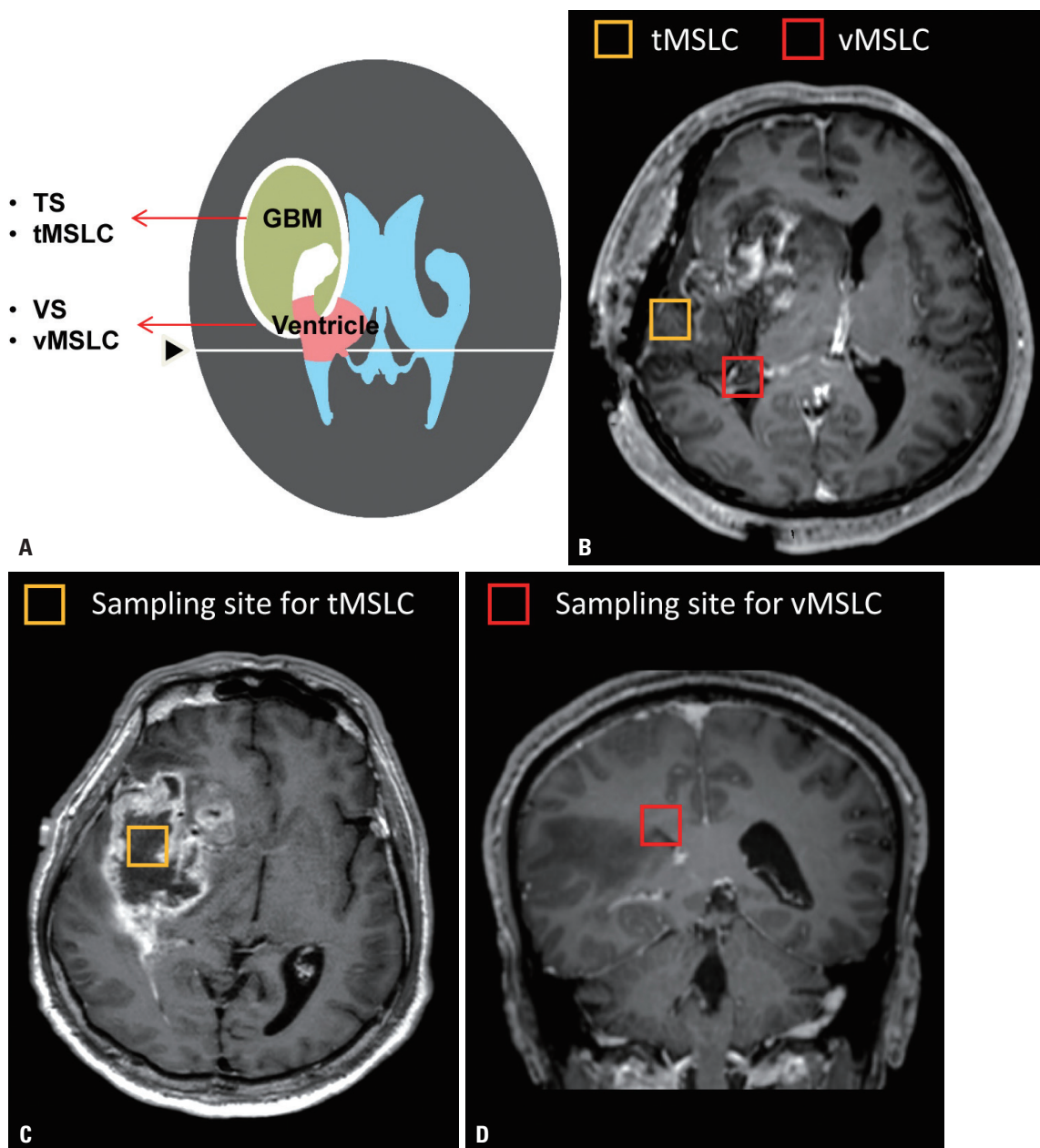


Fig. 1. Isolation of GBM patients-derived cells. (A) Schematic diagram of brain anatomy and cell isolation. TSs and tMSLCs were isolated from the tumor region (yellow), and VSs and vMSLCs were isolated from the trigone of the lateral ventricle region (red). (B-D) Representative T1 contrast-enhanced MR images obtained from case 13–15. (B) Postoperative axial image. (C) Preoperative axial image. (D) Preoperative coronal image. tMSLC, tumor-derived mesenchymal stem-like cell; vMSLC, ventricle-derived mesenchymal stem-like cell; TS, tumorsphere; VS, ventricle sphere; GBM, glioblastoma.

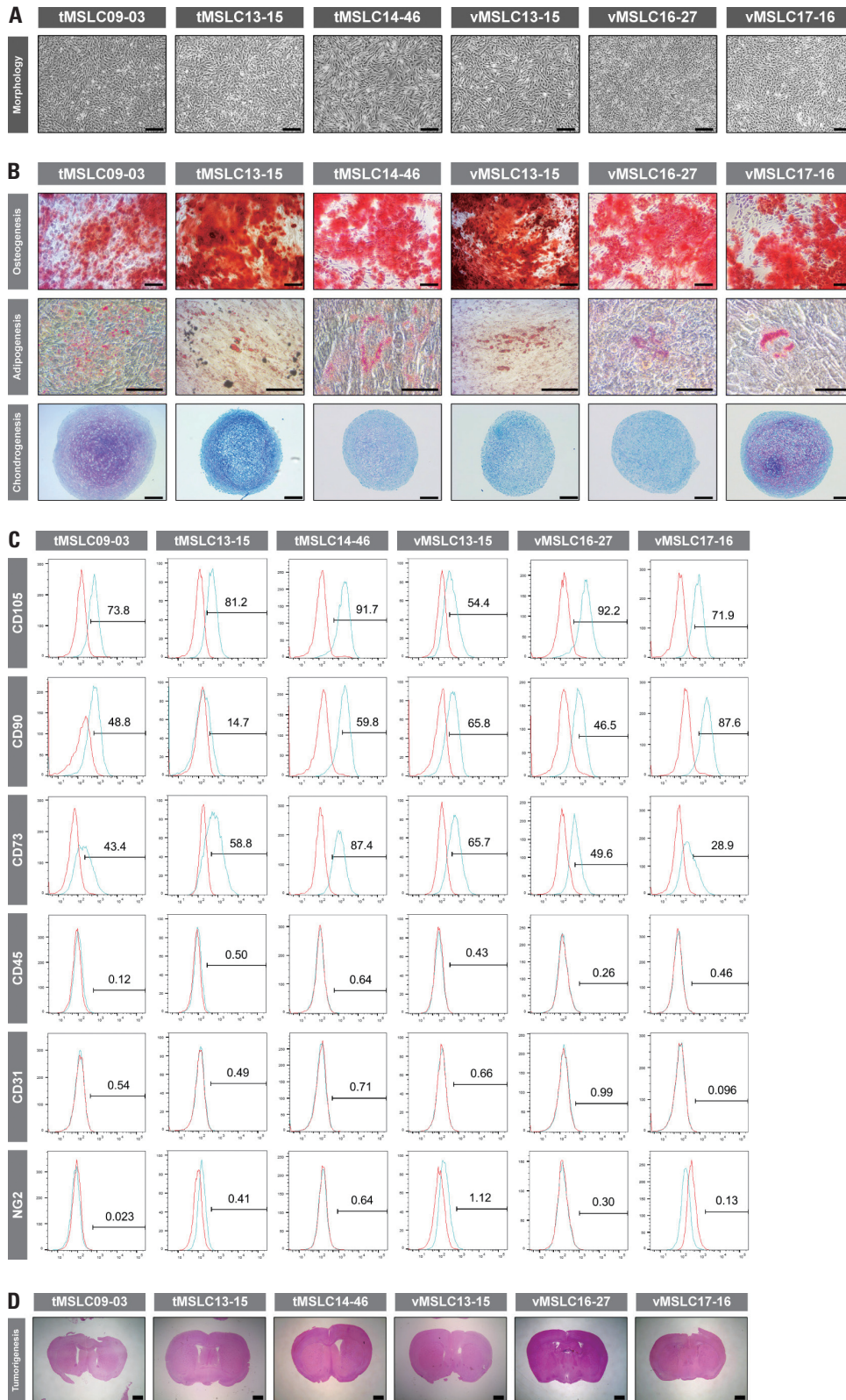


Fig. 2. Characterization of tMSLCs and vMSLCs. (A) Morphology of MSLCs were captured under MSC culture conditions (scale bar=500 μ m). (B) Under trilineage differentiation condition, calcium deposition was stained with Alizarin Red (upper panel), intracellular lipid droplets were stained with Oil Red O (middle panel), and proteoglycans and glycosaminoglycans in the pellet were stained with Toluidine Blue (lower panel). Scale bar=200 μ m. (C) Expressions of surface antigens were evaluated by flow cytometry for mesenchymal (CD105, CD90, and CD73), leukocyte (CD45), endothelial (CD31), and pericyte (NG2) markers. (D) Sections of mouse brains were obtained from euthanized mice at 6 months post-injection of MSLCs and H&E stained to determine tumorigenesis capacity (scale bar=1000 μ m). tMSLC, tumor-derived mesenchymal stem-like cell; vMSLC, ventricle-derived mesenchymal stem-like cell; MSC, mesenchymal stem cell.

gels. Proteins were transferred to nitrocellulose membranes and probed with antibodies against β -catenin (BD Biosciences, San Jose, CA, USA), N-cadherin (R&D Systems, Minneapolis, MN, USA), Zeb1 (Sigma-Aldrich), CD44 (Cell Signaling Technology, Beverly, MA, USA), and GAPDH (Santa Cruz Biotechnology, Santa Cruz, CA, USA). Proteins were detected using horseradish peroxidase-conjugated IgG (Santa Cruz Biotechnology) with Western Lightning Plus-enhanced chemiluminescence reagent (PerkinElmer, Waltham, MA, USA). Images were captured using ImageQuant LAS 4000 mini (GE Healthcare Life Sciences, Little Chalfont, UK). Bands were quantified by densitometry using ImageJ software.

Mouse orthotopic xenograft model

Male athymic nude mice (6 weeks old; Central Lab. Animal Inc., Seoul, Korea) were used in this study. Mice were housed in micro-isolator cages under sterile conditions, and observed for at least 1 week before the study initiation to ensure proper

health. Lighting, temperature, and humidity were controlled centrally. Dissociated GBM TSs (5×10^5 cells/mice; usual cell number for GBM patient-derived TSs) and the same number of tMSCs or vMSCs were implanted into the right frontal lobe of mice at a depth of 4.5 mm using the guide-screw system. If body weight decreased by more than 15% compared to the maximum, mice were euthanized according to the approved protocol. For immunohistochemistry, 5- μ m-thick sections were obtained using a microtome and transferred onto adhesive slides. Antigen retrieval and antibody attachment were performed using an automated instrument (Discovery XT). Zeb1 was detected using a peroxidase/DAB staining system. All experimental procedures involving animals were approved by the Yonsei University College of Medicine Institutional Animal Care and Use Committee (2017-0347). Informed consent was obtained from all individual participants included in the study.

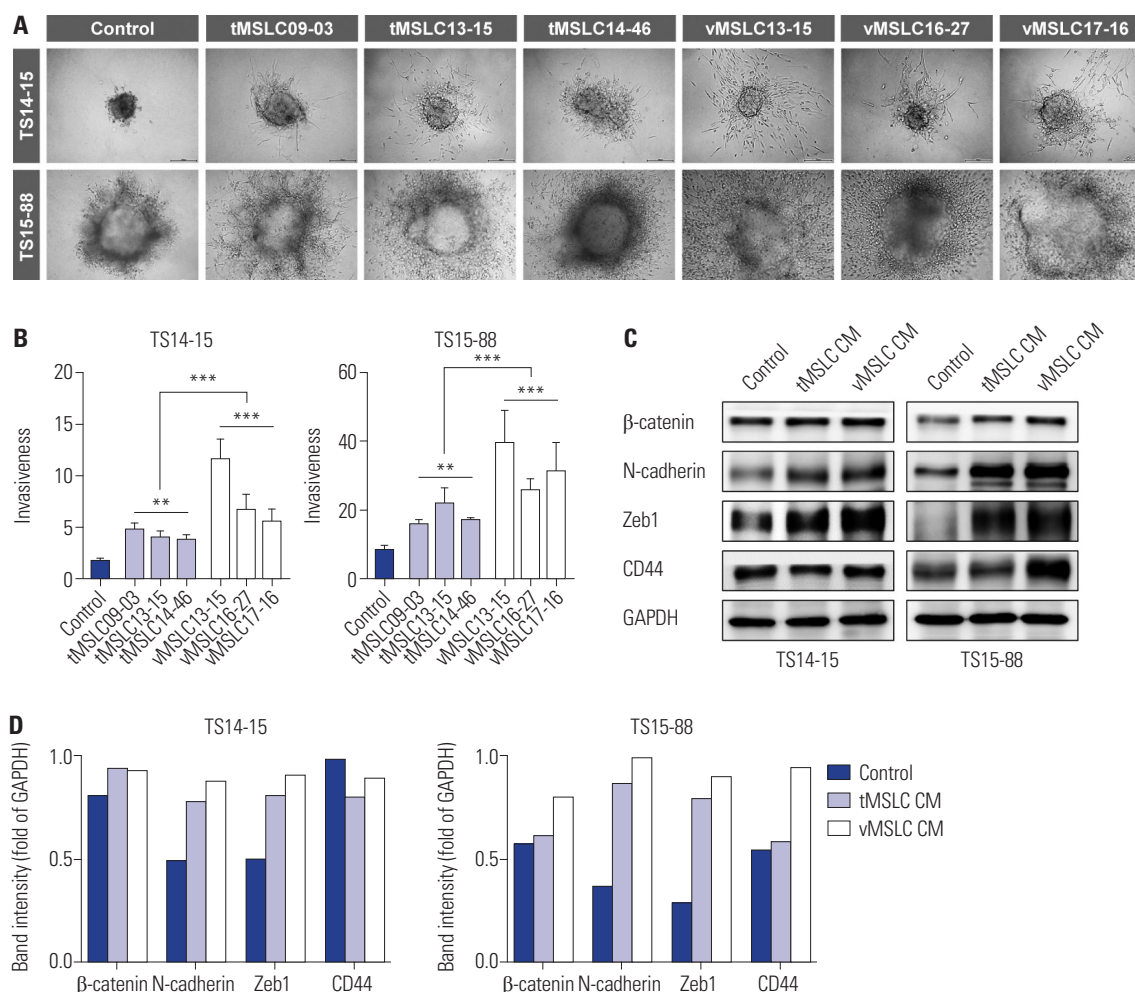


Fig. 3. vMSC-mediated acceleration of invasiveness in GBM TSs. (A and B) Invaded areas were calculated as the increase in occupied area at 72 h relative to that of 0 h, normalized to the initial occupied area [(72 h–0 h)/0 h]. Differences among groups were compared by one-way ANOVA with Tukey's post hoc test for multiple comparisons (** $p < 0.01$, *** $p < 0.001$). (C and D) Proteins were extracted from TS14-15 and TS15-88 cultured with or without MSLC-CM for 48 h. Expression levels of invasion-associated proteins were assessed by western blotting. Band intensities were quantified densitometrically and normalized to GAPDH expression. tMSC, tumor-derived mesenchymal stem-like cell; vMSC, ventricle-derived mesenchymal stem-like cell; TS, tumorsphere; GBM, glioblastoma; CM, conditioned media.

RESULTS

Isolation and characterization of GBM patient-derived cells

To evaluate the effects of vMSCs on GBM, we isolated several types of GBM patient-derived cells, including TSs (n=2) and tMSCs (n=3) from the tumor region of GBM patients, and VSs (n=1) and vMSCs (n=3) from the trigone of the lateral ventricle region (Fig. 1 and Table 1). We next characterized tMSCs and vMSCs to determine whether they showed typical characteristics of human MSCs.²⁹ Both cell types were spindle shaped and adherent to plastic, with an overall morphology similar to that of MSCs (Fig. 2A). Upon culture in tri-lineage-inducing media, these cells underwent osteogenesis, adipogenesis, and chondrogenesis, indicating their human MSC-like mesenchymal differentiation capacity (Fig. 2B). Although no common pathognomonic markers for human MSCs are available, it is generally agreed that MSCs are positive for CD105, CD90, and CD73, and negative for CD45.^{17,29} Both MSLC types met these surface marker criteria (Fig. 2C). Since MSCs from normal mouse brains and glioma xenografts are

located around the vessels,³⁰ we also sought to determine their relationship to perivascular cells by evaluating the expression of CD31 (endothelial marker) and NG2 (pericyte/smooth muscle cell marker). Both MSLC types were negative for CD31 and NG2 (Fig. 2C). Notably, both types of stromal cells lacked tumorigenesis capacity in an in vivo mouse orthotopic xenograft model, distinguishing these cells from tumor cells such as GBM TSs (Fig. 2D). These data suggest that tMSCs and vMSCs have characteristics that are very similar to those of human MSCs in terms of morphology, differentiation capacity, expression of surface markers, and absence of tumorigenesis capacity.

vMSC-induced acceleration of invasion in GBM TSs and VSs

To assess the effects of vMSCs on the invasiveness of GBM TSs, we first collected CM from MSLC-cultured dishes. We then compared the invasiveness of GBM TSs using collagen-based 3D invasion assays in the presence or absence of MSLC-CM (Fig. 3A). In TSs derived from both case 14-15 (TS14-15) and case 15-88 (TS15-88), tMSC-CM significantly enhanced in-

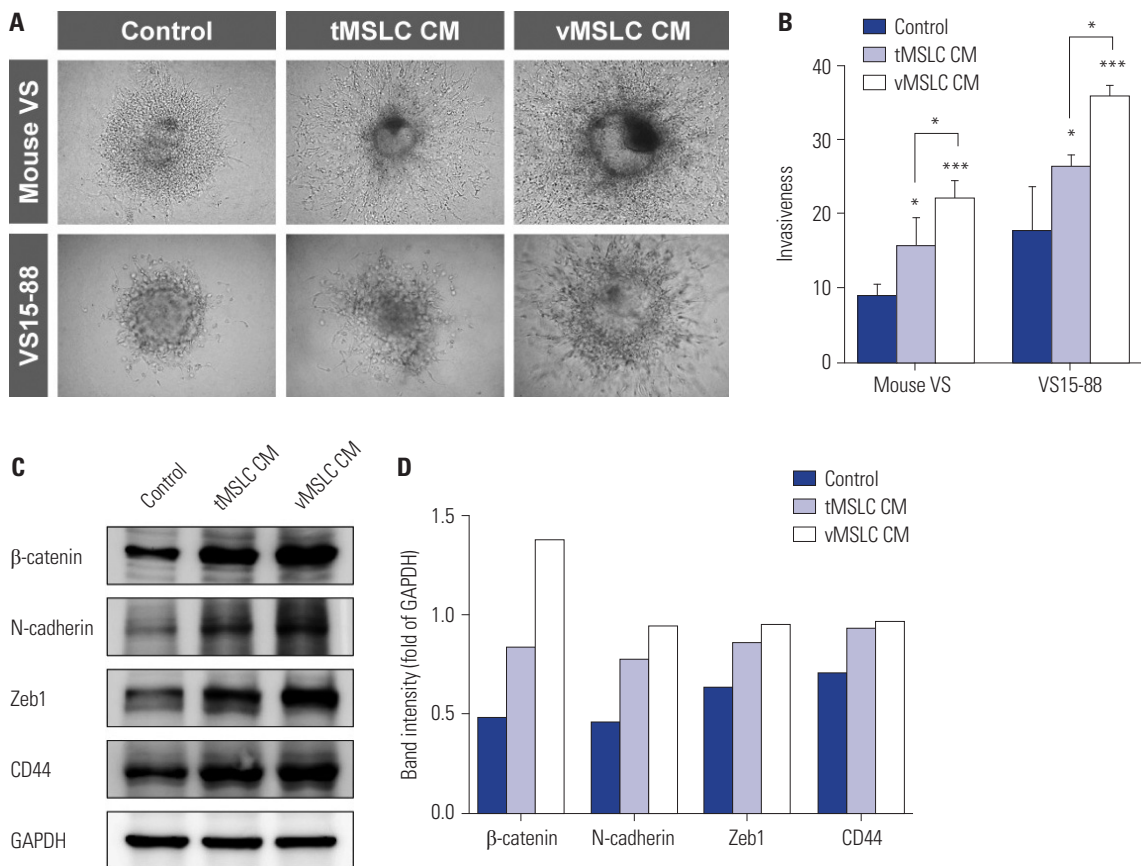


Fig. 4. vMSC-mediated acceleration of invasiveness in GBM VSs. (A and B) Invaded areas were calculated as the increase in occupied area at 72 h relative to that of 0 h, normalized to the initial occupied area [(72 h–0 h)/0 h]. Differences among groups were compared by one-way ANOVA with Tukey’s post hoc test for multiple comparisons (**p*<0.05, ****p*<0.001). (C and D) Proteins were extracted from VS15-88 cultured with or without MSLC-CM for 48 h. Expression levels of invasion-associated proteins were assessed by western blotting. Band intensities were quantified densitometrically and normalized to GAPDH expression. tMSC, tumor-derived mesenchymal stem-like cell; vMSC, ventricle-derived mesenchymal stem-like cell; VS, ventricle sphere; GBM, glioblastoma; CM, conditioned media.

vasiveness compared with the control, whereas vMSLC-CM enhanced invasion to an even greater extent. Three different tMSLC (case 09-03, 13-15, 14-46) and vMSLC (case 13-15, 16-

27, 17-16) isolates showed consistent patterns, indicative of strong vMSLC-mediated acceleration of invasion in GBM TSs (Fig. 3B). Western blotting showed augmented expression of

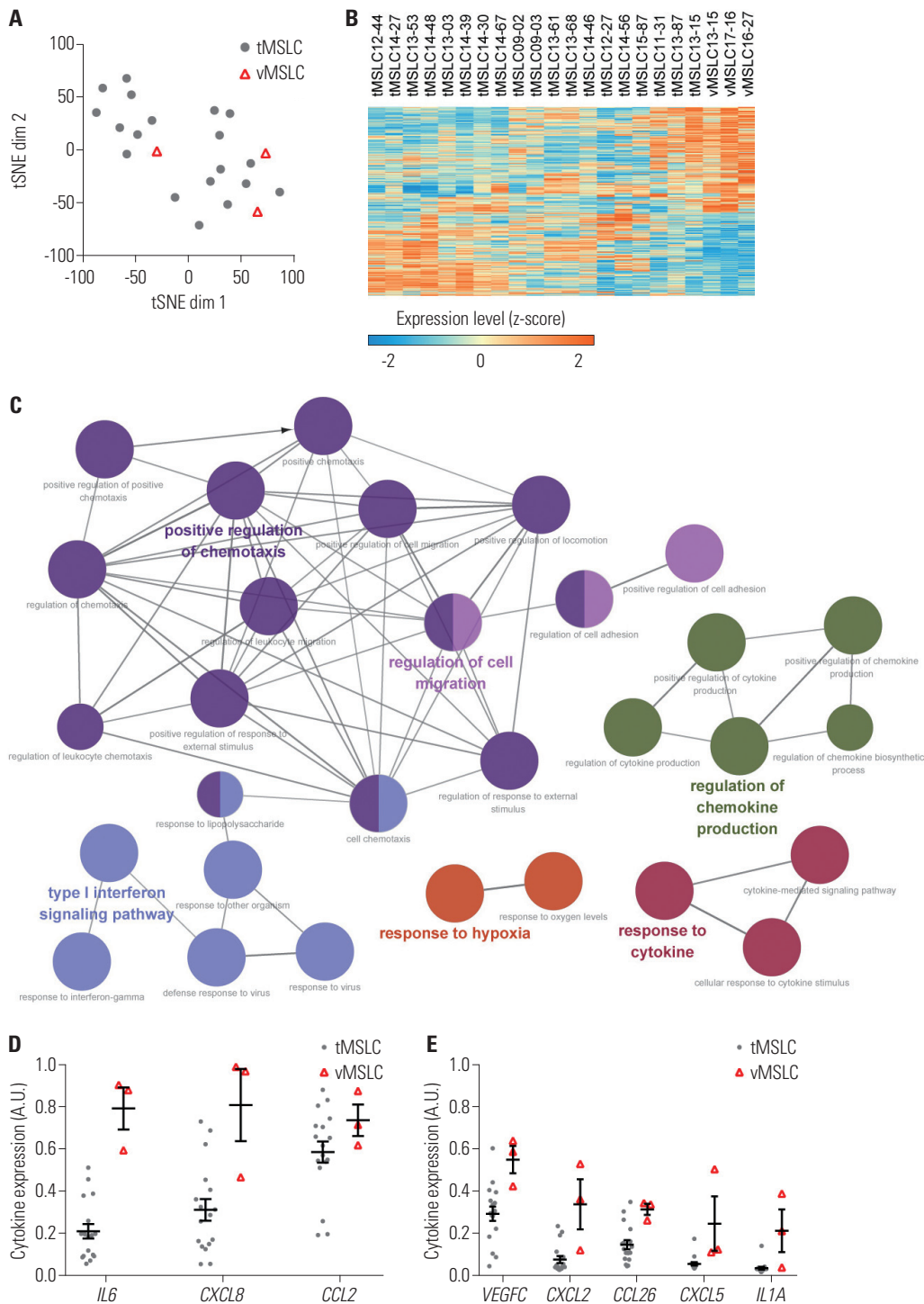


Fig. 5. Gene expression profiles of tMSLCs and vMSLCs. (A) Gene expression profiles of tMSLCs and vMSLCs were obtained from microarray. Unsupervised clustering was performed using the tSNE method. (B) Expression levels of 643 DEGs between tMSLCs and vMSLCs (two-tailed Student's t-test, FDR<5%) are displayed as a heat map. (C) A total of 362 vMSLC-upregulated genes were functionally annotated, clustered, and visualized as an enrichment map. Each node represents a gene ontology (GO) term, with the node size reflecting the statistical significance of over-representation. The edge between two nodes denotes the kappa score relationship. Node colors reflect clustered modules; labels for the most significant GO terms for each module are highlighted. (D and E) Several cytokines with significantly higher expression levels in vMSLCs than tMSLCs (two-tailed Student's t-test, FDR<5%) are presented as dot plots. tMSLC, tumor-derived mesenchymal stem-like cell; vMSLC, ventricle-derived mesenchymal stem-like cell; DEG, differentially expressed gene.

invasion-associated proteins in response to tMSLC-CM and even greater augmentation in response to vMSLC-CM, consistent with 3D invasion assays (Fig. 3C and D). vMSLC-CM also significantly increased the invasiveness of mouse VS and human VS (VS15-88) to a greater extent than tMSLC-CM or control groups, implying that MSLC-secreted factors, especially from vMSLCs, can cause VSs to acquire an infiltrative phenotype, reflecting their shared physiological location (Fig. 4A and B). Consistent with functional assays, western blotting of VS15-88 showed augmented expression of invasion-associated proteins in response to tMSLC-CM and even greater augmentation in response to vMSLC-CM (Fig. 4C and D). These data suggest that vMSLCs accelerate the invasiveness of GBM TSs and VSs.

Transcriptome analysis of vMSLCs

To elucidate the molecular mechanisms underlying the invasion-promoting effects of vMSLCs, we analyzed the gene expression profiles of tMSLCs and vMSLCs using microarrays.³¹ Unsupervised clustering using the tSNE method showed that whole-gene expression profiles were similar between tMSLCs and vMSLCs (Fig. 5A). Therefore, we analyzed 643 differentially expressed genes between tMSLCs and vMSLCs (Fig. 5B). Among them, 362 vMSLC-upregulated genes were significantly enriched in gene sets closely related to invasiveness, including those associated with cell migration, chemokine production, and chemotaxis (Fig. 5C). Specifically, several cytokines investigated in our previous study,²⁰ including *IL6*, *CXCL8*, and *CCL2*, showed significantly higher expression levels in vMSLCs than tMSLCs (Fig. 5D). In addition, other cytokines that are associated with chemotaxis, migration, and invasion, including *VEGFC*, *CXCL2*, *CCL2*, *CXCL5*, and *IL1A*, showed significantly higher expression levels in vMSLCs than tMSLCs (Fig. 5E). These results imply that several chemokines secreted by vMSLCs contribute to the invasiveness of GBM TSs and VSs.

Validation in a mouse orthotopic xenograft model

For in vivo validation of the invasion-promoting effects of vMSLCs, we used a mouse orthotopic xenograft model. Each mouse was implanted with GBM TSs (TS15-88), together with tMSLCs or vMSLCs, and invasiveness relative to the TS-only implanted group was determined based on immunostaining for Zeb1 (Fig. 6A). The TS+vMSLC group showed a significantly greater invaded area compared to the TS only and TS+tMSLC groups (Fig. 6B), recapitulating results from in vitro 3D invasion assays.

DISCUSSION

Cancer treatment strategies have commonly focused on the tumor parenchyma itself. However, considered as an organ, the tumor contains not only proliferating cancer cells, but also diverse non-tumor stromal cells, such as fibroblasts, macrophages, and endothelial cells, that establish crosstalk with each other. In the present study, we provide the first characterization of GBM patient-derived vMSLCs in both functional and molecular terms, identifying these cells as stromal interaction partners of GBM.

The detection of MSLCs in the tumor microenvironment has raised interest in their role in tumor progression. However, the evidences on this point are often contradictory, presumably owing to differences in the origin and type of tumors.^{32,33} The SVZ was recently proposed as the region of cellular origin of GBM,^{23,24} notwithstanding the fact that cells in the SVZ are pathologically normal. Since vMSLCs are derived from this region, it is possible to infer that the interactions between vMSLCs and potential GBM cells-of-origin are physiologically reasonable. Although intermediary steps and molecular processes from cell-of-origin to GBM remain to be elucidated, vMSLC-

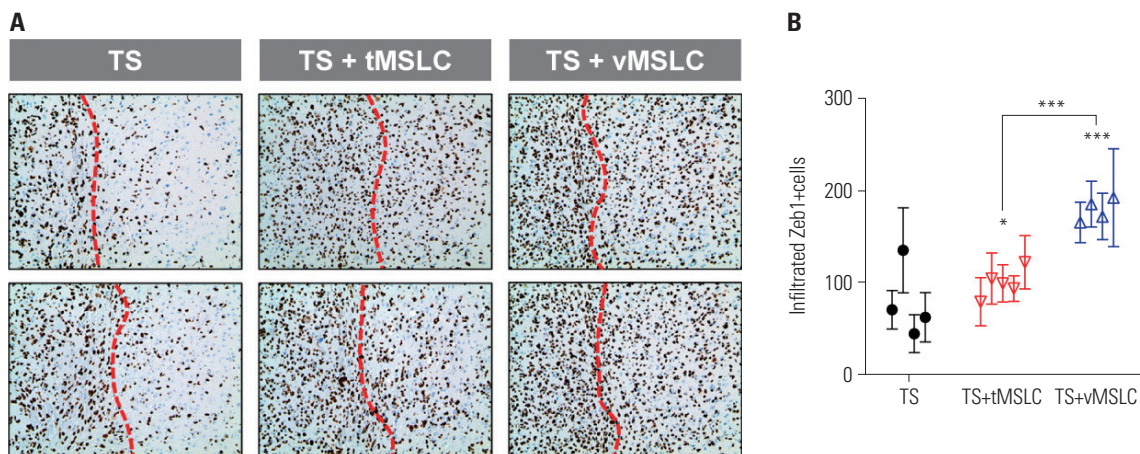


Fig. 6. Invasion-promoting effects of vMSLCs in mouse orthotopic xenograft models. (A) Representative images of sections of brains obtained from euthanized mice immunostained for Zeb1 (brown) to identify invading cells. For all images, nuclei were counterstained with hematoxylin (blue). (B) The number of infiltrated Zeb1+ cells [right side of red dashed line in (A)], determined from 10 images captured for each mouse, was counted for each group (one-way ANOVA with Tukey's post hoc test for multiple comparisons; * $p < 0.05$, *** $p < 0.001$). tMSLC, tumor-derived mesenchymal stem-like cell; vMSLC, ventricle-derived mesenchymal stem-like cell; TS, tumorsphere.

mediated acquisition of an infiltrative phenotype in the SVZ and subsequent movement to the cortex region to form the GBM mass could be a plausible scenario. The vMSLC-mediated acceleration of invasiveness in mouse and human VSs as well as GBM TSs (Fig. 4) supports this idea.

The invasive capabilities of tumors, together with mesenchymal transition and distant metastasis, are hallmarks of most solid tumors.³⁴ Invasiveness is a major challenge in the clinical management of GBM patients.^{6,35} In addition, our previous research showed that the invasive subtype of GBM is associated with a worse prognosis than the mitotic subtype,³⁶ suggesting that invasiveness could be a robust classifier of GBM that reflects biological phenotype and patient prognosis, despite the intertumoral heterogeneity of GBM. However, no therapeutic interventions targeting invasion are available for the treatment of GBM patients. Despite the enormous efforts devoted to developing targeted therapies for GBM, no chemical agents are available for GBM patients except temozolomide (TMZ), a cytotoxic agent that causes several side effects. We propose that targeting vMSLCs and vMSLC-secreted cytokines would constitute a novel invasion-inhibiting therapeutic strategy.

The goals of future studies are to develop and assess vMSLC-targeting therapeutic strategies for GBM. Prudence should guide attempts to increase the extent of resection (EOR) in GBM patients, owing to the anatomical and functional characteristics of the brain. Since targeting invasiveness through vMSLC could definitize the margin between the tumor and normal regions, it can be utilized as a neoadjuvant therapy to maximize EOR and reduce the probability of recurrence. In addition, vMSLCs could act as boosters of GBM progression at the region where GBM genesis originates. Given this originating region, vMSLC-targeted therapeutics could suppress re-invasion of GBM cells-of-origin into cortex regions and prevent subsequent relapse. Importantly, this therapy could be combined with other therapeutic modalities, including TMZ and radiotherapy, avoiding overlapping of action mechanisms. Future works with larger number of ventricle-associated samples are required to develop precise therapeutic strategies and evaluate the relationship with pharmacogenomic markers, such as methylation patterns of *MGMT* promoter regions.³⁷

ACKNOWLEDGEMENTS

This work was supported by the National Research Foundation of Korea (NRF) grant funded by the Korean government, including the Ministry of Science and ICT (NRF-2022R1A2B5B03001199, NRF-2020M2D9A2092372, NRF-2020M3E5E2037960, NRF-2017R1C1B2003686) and the Ministry of Education (NRF-2021R1I1A1A01048717). This work was also supported by the Team Science Award grant from Yonsei University College of Medicine (6-2021-0192).

AUTHOR CONTRIBUTIONS

Conceptualization: Junseong Park and Seok-Gu Kang. **Data curation:** Junseong Park and Dongkyu Lee. **Formal analysis:** Junseong Park. **Funding acquisition:** Junseong Park and Seok-Gu Kang. **Investigation:** Junseong Park. **Methodology:** Junseong Park, Dongkyu Lee, Jin-Kyoung Shim, and Seon-Jin Yoon. **Project administration:** Seok-Gu Kang. **Resources:** Ju Hyung Moon, Eui Hyun Kim, Jong Hee Chang, and Su-Jae Lee. **Software:** Junseong Park. **Validation:** Junseong Park, Dongkyu Lee, and Jin-Kyoung Shim. **Visualization:** Junseong Park, Dongkyu Lee, and Seon-Jin Yoon. **Writing—original draft preparation:** Junseong Park. **Writing—review and editing:** Seok-Gu Kang. **Approval of final manuscript:** all authors.

ORCID iDs

Junseong Park	https://orcid.org/0000-0003-0436-8614
Dongkyu Lee	https://orcid.org/0000-0002-0241-1554
Jin-Kyoung Shim	https://orcid.org/0000-0003-3819-0180
Seon-Jin Yoon	https://orcid.org/0000-0002-3255-5081
Ju Hyung Moon	https://orcid.org/0000-0002-8925-5821
Eui Hyun Kim	https://orcid.org/0000-0002-2523-7122
Jong Hee Chang	https://orcid.org/0000-0003-1509-9800
Su-Jae Lee	https://orcid.org/0000-0002-4023-4819
Seok-Gu Kang	https://orcid.org/0000-0001-5676-2037

REFERENCES

- Hoshida R, Jandial R. 2016 World Health Organization classification of central nervous system tumors: an era of molecular biology. *World Neurosurg* 2016;94:561-2.
- Stupp R, Hegi ME, Mason WP, van den Bent MJ, Taphoorn MJ, Janzer RC, et al. Effects of radiotherapy with concomitant and adjuvant temozolomide versus radiotherapy alone on survival in glioblastoma in a randomised phase III study: 5-year analysis of the EORTC-NCIC trial. *Lancet Oncol* 2009;10:459-66.
- Roh TH, Park HH, Kang SG, Moon JH, Kim EH, Hong CK, et al. Long-term outcomes of concomitant chemoradiotherapy with temozolomide for newly diagnosed glioblastoma patients: a single-center analysis. *Medicine (Baltimore)* 2017;96:e7422.
- Roh TH, Kang SG, Moon JH, Sung KS, Park HH, Kim SH, et al. Survival benefit of lobectomy over gross-total resection without lobectomy in cases of glioblastoma in the noneloquent area: a retrospective study. *J Neurosurg* 2020;132:895-901.
- Auffinger B, Spencer D, Pytel P, Ahmed AU, Lesniak MS. The role of glioma stem cells in chemotherapy resistance and glioblastoma multiforme recurrence. *Expert Rev Neurother* 2015;15:741-52.
- Jeong H, Park J, Shim JK, Lee JE, Kim NH, Kim HS, et al. Combined treatment with 2'-hydroxycinnamaldehyde and temozolomide suppresses glioblastoma tumorspheres by decreasing stemness and invasiveness. *J Neurooncol* 2019;143:69-77.
- Jackson M, Hassiotou F, Nowak A. Glioblastoma stem-like cells: at the root of tumor recurrence and a therapeutic target. *Carcinogenesis* 2015;36:177-85.
- Kang SG, Cheong JH, Huh YM, Kim EH, Kim SH, Chang JH. Potential use of glioblastoma tumorsphere: clinical credentialing. *Arch Pharm Res* 2015;38:402-7.
- Patrizii M, Bartucci M, Pine SR, Sabaawy HE. Utility of glioblastoma patient-derived orthotopic xenografts in drug discovery and personalized therapy. *Front Oncol* 2018;8:23.
- Kong BH, Park NR, Shim JK, Kim BK, Shin HJ, Lee JH, et al. Isolation of glioma cancer stem cells in relation to histological grades in

- glioma specimens. *Childs Nerv Syst* 2013;29:217-29.
11. Kim KM, Shim JK, Chang JH, Lee JH, Kim SH, Choi J, et al. Failure of a patient-derived xenograft for brain tumor model prepared by implantation of tissue fragments. *Cancer Cell Int* 2016;16:43.
 12. Park J, Shim JK, Kang JH, Choi J, Chang JH, Kim SY, et al. Regulation of bioenergetics through dual inhibition of aldehyde dehydrogenase and mitochondrial complex I suppresses glioblastoma tumorspheres. *Neuro Oncol* 2018;20:954-65.
 13. Thomas AA, Brennan CW, DeAngelis LM, Omuro AM. Emerging therapies for glioblastoma. *JAMA Neurol* 2014;71:1437-44.
 14. Behnan J, Isakson P, Joel M, Cilio C, Langmoen IA, Vik-Mo EO, et al. Recruited brain tumor-derived mesenchymal stem cells contribute to brain tumor progression. *Stem Cells* 2014;32:1110-23.
 15. Li L, Cole J, Margolin DA. Cancer stem cell and stromal microenvironment. *Ochsner J* 2013;13:109-18.
 16. Valkenburg KC, de Groot AE, Pienta KJ. Targeting the tumour stroma to improve cancer therapy. *Nat Rev Clin Oncol* 2018;15:366-81.
 17. Kim YG, Jeon S, Sin GY, Shim JK, Kim BK, Shin HJ, et al. Existence of glioma stroma mesenchymal stemlike cells in Korean glioma specimens. *Childs Nerv Syst* 2013;29:549-63.
 18. Kong BH, Shin HD, Kim SH, Mok HS, Shim JK, Lee JH, et al. Increased in vivo angiogenic effect of glioma stromal mesenchymal stem-like cells on glioma cancer stem cells from patients with glioblastoma. *Int J Oncol* 2013;42:1754-62.
 19. Lim EJ, Suh Y, Yoo KC, Lee JH, Kim IG, Kim MJ, et al. Tumor-associated mesenchymal stem-like cells provide extracellular signaling cue for invasiveness of glioblastoma cells. *Oncotarget* 2017;8:1438-48.
 20. Lim EJ, Kim S, Oh Y, Suh Y, Kaushik N, Lee JH, et al. Crosstalk between GBM cells and mesenchymal stemlike cells promotes the invasiveness of GBM through the C5a/p38/ZEB1 axis. *Neuro Oncol* 2020;22:1452-62.
 21. Yoon SJ, Shim JK, Chang JH, Moon JH, Roh TH, Sung KS, et al. Tumor mesenchymal stem-like cell as a prognostic marker in primary glioblastoma. *Stem Cells Int* 2016;2016:6756983.
 22. Moon JH, Kim SH, Shim JK, Roh TH, Sung KS, Lee JH, et al. Histopathological implications of ventricle wall 5-aminolevulinic acid-induced fluorescence in the absence of tumor involvement on magnetic resonance images. *Oncol Rep* 2016;36:837-44.
 23. Lee JH, Lee JE, Kahng JY, Kim SH, Park JS, Yoon SJ, et al. Human glioblastoma arises from subventricular zone cells with low-level driver mutations. *Nature* 2018;560:243-7.
 24. Yoon SJ, Park J, Jang DS, Kim HJ, Lee JH, Jo E, et al. Glioblastoma cellular origin and the firework pattern of cancer genesis from the subventricular zone. *J Korean Neurosurg Soc* 2020;63:26-33.
 25. Oh HC, Shim JK, Park J, Lee JH, Choi RJ, Kim NH, et al. Combined effects of niclosamide and temozolomide against human glioblastoma tumorspheres. *J Cancer Res Clin Oncol* 2020;146:2817-28.
 26. Kim EH, Lee JH, Oh Y, Koh I, Shim JK, Park J, et al. Inhibition of glioblastoma tumorspheres by combined treatment with 2-deoxyglucose and metformin. *Neuro Oncol* 2017;19:197-207.
 27. Du P, Kibbe WA, Lin SM. Lumi: a pipeline for processing Illumina microarray. *Bioinformatics* 2008;24:1547-8.
 28. Bindea G, Mlecnik B, Hackl H, Charoentong P, Tosolini M, Kirilovsky A, et al. ClueGO: a Cytoscape plug-in to decipher functionally grouped gene ontology and pathway annotation networks. *Bioinformatics* 2009;25:1091-3.
 29. Dominici M, Le Blanc K, Mueller I, Slaper-Cortenbach I, Marini F, Krause D, et al. Minimal criteria for defining multipotent mesenchymal stromal cells. The international society for cellular therapy position statement. *Cytotherapy* 2006;8:315-7.
 30. Kang SG, Shinjima N, Hossain A, Gumin J, Yong RL, Colman H, et al. Isolation and perivascular localization of mesenchymal stem cells from mouse brain. *Neurosurgery* 2010;67:711-20.
 31. Lee J, Park J, Choi C. Identification of phenotype deterministic genes using systemic analysis of transcriptional response. *Sci Rep* 2014;4:4413.
 32. Karnoub AE, Dash AB, Vo AP, Sullivan A, Brooks MW, Bell GW, et al. Mesenchymal stem cells within tumour stroma promote breast cancer metastasis. *Nature* 2007;449:557-63.
 33. Shinagawa K, Kitadai Y, Tanaka M, Sumida T, Kodama M, Higashi Y, et al. Mesenchymal stem cells enhance growth and metastasis of colon cancer. *Int J Cancer* 2010;127:2323-33.
 34. Hanahan D, Weinberg RA. Hallmarks of cancer: the next generation. *Cell* 2011;144:646-74.
 35. Kwiatkowska A, Symons M. Signaling determinants of glioma cell invasion. *Adv Exp Med Biol* 2020;1202:129-49.
 36. Park J, Shim JK, Yoon SJ, Kim SH, Chang JH, Kang SG. Transcriptome profiling-based identification of prognostic subtypes and multi-omics signatures of glioblastoma. *Sci Rep* 2019;9:10555.
 37. Brandes AA, Franceschi E, Tosoni A, Blatt V, Pession A, Tallini G, et al. MGMT promoter methylation status can predict the incidence and outcome of pseudoprogression after concomitant radiochemotherapy in newly diagnosed glioblastoma patients. *J Clin Oncol* 2008;26:2192-7.